PAPER

Check for updates

Prediction of Acid Red 138 solubility in supercritical CO_2 with water co-solvent†

Fang Ye,[a] Yuping Zhao,[a] Zhiping Mao,[a] Laijiu Zheng,[a] Huanda Zheng [ID] *[a]
and Huizhen Ke*[b]

Acid Red 138, as a weak acid azo dye with a long alkyl chain, is widely used for protein fiber dyeing while it cannot dissolve in supercritical carbon dioxide. The objective of this study is to investigate the solubility of Acid Red 138 with water at the temperatures of 353.15, 363.15, 373.15, 393.15 and 413.15 K and over a pressure range of 20 to 26 MPa. The test results revealed that the phase equilibrium of water and Acid Red 138 was affected by the competition between pressure and density of supercritical carbon dioxide. Furthermore, the experimental solubilities were correlated by three types of density-based model. Good agreement with less than 3.36% of average absolute relative deviation between the calculated and the experimental data of water was achieved. In addition, the Chrastil model, Mendez–Santiago–Teja model and Sung–Shim model exhibited excellent correlation results for Acid Red 138 solubilities with the AARD values of 8.58%, 6.06% and 5.19%. Better understanding of the solubility behavior of Acid Red 138 in supercritical carbon dioxide displays potential for developing a microemulsion system for the eco-friendly dyeing of natural fibers.

1 Introduction

Carbon dioxide in a supercritical state has received extensive attention due to its low cost and wide availability, and moderate critical conditions of 304.15 K and 7.38 MPa.[1,2] As a green solvent, one of the major benefits of supercritical carbon dioxide results from the unique viscosity, density and diffusivity which presents the properties of a liquid and a gas, and can be controlled by varying temperature and pressure.[3] With the characteristics above, supercritical carbon dioxide is expected to be an novel eco-friendly solvent which is currently employed in numerous industrial fields, such as dyeing, chemical reactions, extraction, separation and so on.[4–6] However, there are still a series of hurdles to using supercritical carbon dioxide mainly resulting from its inability to dissolve the substances with hydrophilicity or high molecular weight, for example, natural fibers, proteins as well as most polymers and dyes because of the comparatively low polarity and dielectric constant.[7] A strategy that adds co-solvents into supercritical carbon dioxide is developed accordingly to increase the poor dissolving capacity of solutes. Of all the co-solvents, water is one of the most common used to improve the polarity of carbon

dioxide, and plays significant roles in numerous supercritical processes.[8,9]

The application of supercritical carbon dioxide in the textile field has also shown its advantage for replacing the environmentally unfriendly aqueous dyeing process because of the low energy consumption and zero waste water emission.[10–14] Former experiments verified that during supercritical carbon dioxide dyeing process, the addition of water always performs the improvement effects for natural fibers dyeing. Firstly, a certain amount of water in supercritical carbon dioxide can alter the chemical nature (polarity and pH) of the fluid, thus affecting the solubility and reactivity of dyes.[15] Secondly, water can break up the hydrogen bonds between the macromolecular chains of natural fibers, and form hydrogen bonds with the hydroxyl and/or amine groups, swelling the fibers and improving the dyeability.[16] In addition, using water as a co-solvent of supercritical carbon dioxide has also been proved to be effectively employed in the cleaning for oil, rabbit skin glue, beetroot paste and *Aspergillus niger* fungi on textiles.[17] Nevertheless, water also brings in some opposite effects. On the one hand, acidic condition of supercritical carbon dioxide will be strengthened by adding water, which can lead to the increase of the short fiber content of protein fibers.[18] On the other hand, water concentration can also increase the uniform or localize corrosion rates, which results in the corrosion of mild steel in supercritical fluid apparatus.[19]

To use water as a co-solvent, it appears to be particularly important to be able to determine the amount of water in a specific temperature and pressure for a supercritical carbon

[a]Liaoning Provincial Key Laboratory of Ecological Textile, Dalian Polytechnic University, Dalian 116034, Liaoning, China. E-mail: zhenghd@dlpu.edu.cn; Fax: +86-411-86323438; Tel: +86-411-86318763

[b]Fujian Key Laboratory of Novel Functional Textile Fibers and Materials (Minjiang University), Fuzhou, Fujian, 350108, China. E-mail: kehuizhen2013@163.com

† Electronic supplementary information (ESI) available. See DOI: 10.1039/c9ra06749c

dioxide process design.[20] King studied the solubility between water and carbon dioxide from 5 to 20 MPa and 288.15 to 313.15 K, and reported the solubilities of water in supercritical carbon dioxide were less than 0.006 mol%.[21] Tabasinejad obtained the water solubility from 422 to 483 K over a wide range of 3.6 to 134 MPa, and found the maximum could be reached to 47.02 mol% in supercritical carbon dioxide.[22] For supercritical carbon dioxide dyeing, it always requires higher temperature (≥353.15 K) and pressure (≥18 MPa) ranges in comparison to extraction and other industrial fields. Under these conditions, water content will be varied, thus resulting in the significant changes for the application properties of supercritical carbon dioxide, fibers, dyes as well as dyeing apparatus. Generally, it is extremely difficult for cotton and wool to be dyed since acid dyes and other high polar dyes cannot be dissolved in supercritical carbon dioxide. Some researches have shown that dye solubility enhancement will occur in supercritical carbon dioxide with ethanol, acetone, DMSO and ionic liquids as co-solvents.[23,24] Özcan reported that Acid Red 57/dodecyltrimethylammonium bromide can dissolve in methanol modified supercritical carbon dioxide by the hydrophobic ion-pairing.[25] Simultaneously, polar dyes can also be dissolved by adding water, thereby improving the dyeing properties of natural fibers.[26] However, so far there are few data reported on the water and high polar dyes solubilities in supercritical carbon dioxide dyeing process. Models that can calculate the water content and dye solubility data under supercritical carbon dioxide dyeing conditions are needed unquestionably.

In this work, the solubilities of water was investigated in supercritical carbon dioxide by employing a phase equilibrium apparatus with temperatures of 353.15 to 413.15 K and pressures of 20 to 26 MPa, respectively. Moreover, as a commonly used dye for protein fibers dyeing, the solubilities of Acid Red 138 were measured in supercritical carbon dioxide with water as co-solvent to determine the influence of water. The solubility data of water and Acid Red 138 with water as co-solvent were also correlated by Chrastil equation, Mendez-Santiago–Teja equation and Sung–Shim equation, respectively.

2 Experimental

2.1 Materials and chemicals

Carbon dioxide with a certified purity of 99.99% was purchased from China Haohua (Dalian) Research & Design Institute of Chemical Industry Co., Ltd. Acid Red 138 (>98%, CAS no. 15792-43-5) was supplied by ZheJiang JiHua Group Co., Ltd (China), used without further purification. Ultra-purified water whose resistivity is 18 MΩ cm was used in the experiments. The detailed information for all the chemical samples is shown in Table 1.

2.2 Equipment and procedures

Solubilities of water and Acid Red 138 were measured by employing a modified SPM Phase Equilibrium System (Waters, US), and the schematic diagram of the apparatus is displayed in Fig. 1. 5 ml distilled water or 0.2 ml Acid Red 138 aqueous solution (10 g l^{-1}) was firstly injected into an equilibrium cell (20 ml) with a sapphire window (3). Liquid carbon dioxide in a gas cylinder (1) was filtered by employing a purifier (2), and then injected into the equilibrium cell at 273.15 K until the cell is filled. Afterwards, carbon dioxide fluid was heated to above 304.15 K by employing an electric heater (4). In such a case, carbon dioxide in supercritical state was reached with the pressure increasing at high temperatures, and the pre-determined condition was obtained. In this system, supercritical carbon dioxide and liquid were stirred adequately by an electromagnetic agitator (5) until the dissolving equilibrium was reached around 120 min according to preliminary experiments. Before the experiments, each absorption cell (6 and 7) was weighed at ambient temperature and pressure with carbon dioxide filled. To prevent the liquid from escaping, the outlet of the absorption cell was equipped with microfilters. According to Maurer's preliminary experiments,[27] the flow rate of the carbon dioxide phase leaving the traps was kept below 4 dm^3 min^{-1}, which plays the most significant impact on the accuracy of the equilibrium data. Thus, after the equilibrium was obtained in the equilibrium cell, the water and/or dyes dissolved in super-critical carbon dioxide were passed into the absorption cells with the flow rate slower than 3 dm^3 min^{-1}. During the collecting process, an ice-cold trap (8) was used to liquefy the solutes fully, and then the absorbing solution was collected for weighing a second time after the absorption cells were heated to atmospheric temperature and pressure. The data shown for each point are averages of three single measurements.

2.3 Quantitative measurement of solubility

To quantitatively measure the solubility data, the weight of water was measured by a METTLER TOLEDO analytical micro-balance before and after supercritical carbon dioxide dissolving. Moreover, a series of standard Acid Red 138 solutions were freshly prepared in water solution. Standard curve of the relationship between the absorbance of Acid Red 138 and its concentration was generated using a PerkinElmer ultraviolet-visible spectrophotometer at the maximum absorbance peak ($\lambda_{max} = 517$ nm), as shown in Fig. 2. The absorption intensity of the absorbing solution was then tested by the ultraviolet-visible spectrophotometer after bring to volume by water in volumetric flask, and the dye concentration can be obtained accordingly.

The solubilities of water and Acid Red 138 under various supercritical carbon dioxide dyeing conditions were determined in terms of the mole fraction (y_2) according to eqn (1) and (2) after the equilibrium was achieved:

$$y_2 = \frac{n_i}{n_{CO_2} + n_1 + \ldots + n_i} = \frac{\frac{m_i}{M_i}}{\frac{m_{CO_2}}{M_{CO_2}} + \frac{m_1}{M_1} + \ldots + \frac{m_i}{M_i}} \quad (1)$$

$$m_1 = \rho V \quad (2)$$

where m_{CO_2} and m_i are the weight of carbon dioxide and solute; n_{CO_2} and n_i are the mole number of carbon dioxide and solute; M_{CO_2} and M_i are the mole mass of carbon dioxide and solute. ρ is

Table 1 Description of chemical samples

Chemical name	CAS	Formula	Molecular weight (g mol^{-1})	Source	Purity^a
Carbon dioxide	124-38-9	CO_2	44.01	Haohua (Dalian)	$x > 0.9999$
Water	7732-18-5	H_2O	18.01	Barnstead Water Purification Systems	DDI (18.24 MΩ cm)
Acid Red 138	15792-43-5	$C_{30}H_{37}N_3Na_2O_8S_2$	677.74	JiHua	$x > 0.98$

^{a} Purity as stated by the supplier; x is mole fraction.

the density of carbon dioxide, which can be obtained from the NIST fluid property database.[28] V are the volume of carbon dioxide.

3 Results and discussion

3.1 Reliability compliance test and the solubility data

To guarantee the reliable solubility data, solubilities of ethylene glycol at different pressures and with a temperature of 353.15 K were tested using the SPM Supercritical Phase Equilibrium System. The measured solubility data of ethylene glycol were compared to the values reported by Jiang.[29] As shown in Table S1,† the obtained results in the SPM Phase Equilibrium System were quantitatively similar to the previous data. Moreover, the relative deviation between our solubility data and the reported results was less than 10%, which proved the accuracy of the Phase Equilibrium System for the solubility test.

On this basis, the solubilities of water and Acid Red 138 with water as co-solvent were measured at temperatures and pressures ranging from 353.15 to 413.15 K and 20 to 26 MPa, and the resulting solubilities have been listed in Tables S2 and S3,† respectively.

3.2 Effect of experimental parameters on the solubilities of water

Effect of carbon dioxide pressure on the mole fraction (y_2) of the water is displayed in Fig. 3. The solubilities of water increased gradually with the rising pressure at a constant system temperature, which presents the typical solubility trends of nonvolatile organic molecules in supercritical carbon dioxide.[30]

The solubility enhanced from 17.52×10^{-3} to 19.69×10^{-3} mol mol^{-1} at 353.15 K with the system pressure elevating from 20 to 26 MPa since the stronger solvent power is formed with higher density of supercritical carbon dioxide at a certain temperature.[28] Moreover, data about water solubility in supercritical carbon dioxide from this study were also compared with previous experimental data. From 353.15 to 373.15 K, our data are slightly larger than those determined by Jiang (8.37–14.14 mol mol^{-1}),[31] and the reason may due to the fact that most of the Jiang's data are obtained at lower temperature. The data of water solubility measured by Wang at 20 MPa (21.1×10^{-3} to 44.4×10^{-3} mol mol^{-1}) are higher than our measurements because of the possibly existing calibration error for the characteristic peaks' relative intensity of Raman spectrum.[32]

Furthermore, Fig. 3 also presents the solubilities of water increased moderately with system temperature increasing at the pressures ranging from 20 to 26 MPa. This is primarily due to the existence of combined action between pressure and density of supercritical carbon dioxide, which ultimately affects the two-phase equilibrium.[19] On the one hand, an increase in temperature increases the saturation vapor pressure of the solute, thereby making the solubility rising; on the other hand, the density of carbon dioxide decreases as the temperature increases, which makes the water less soluble. When the system pressure reaches more than 20 MPa, the effect of pressure on the water solubilities dominates. Thus, the solubilities of water enhanced as temperature increased in supercritical carbon dioxide. The above results demonstrated that the solubilities of water can be improved significantly by regulating the system temperature under higher pressure conditions.
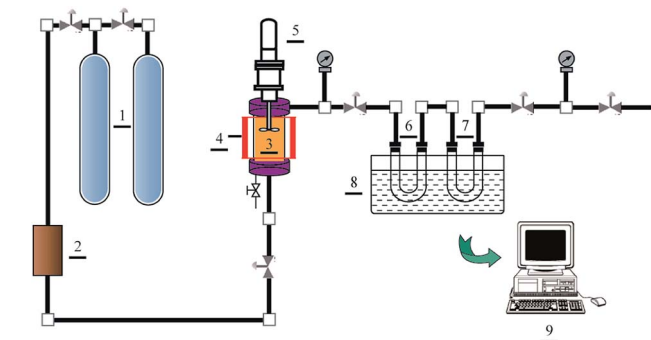

Fig. 1 Phase equilibrium apparatus: (1) gas cylinder, (2) purifier, (3) equilibrium cell, (4) electric heater, (5) electromagnetic agitator, (6 and 7) absorption cell, (8) ice-cold trap, (9) control terminal.
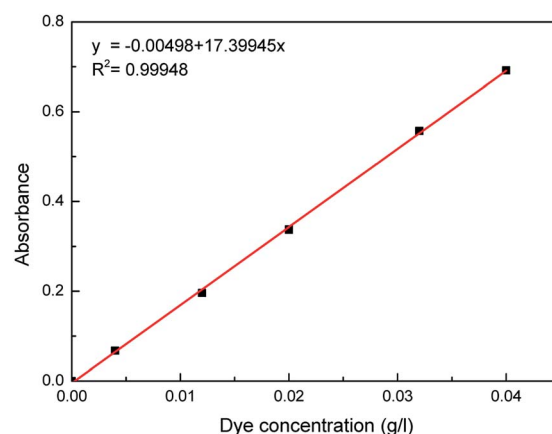

y = -0.00498+17.39945x
R^2= 0.99948

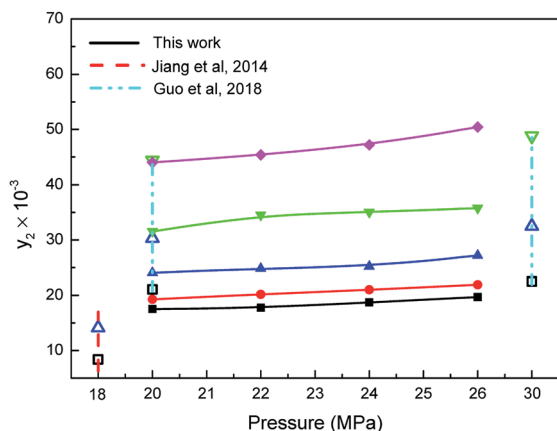**Fig. 2** Standard absorbance–concentration curve of Acid Red 138.

Fig. 3 Relationship between the solubilities of water and the pressure: ■, □ -353.15 K, ● -363.15 K, ▲, △ -373.15 K, ▼, ▽ -393.15 K, ◆ -413.15 K.

Table 2 Parameters of Chrastil model, Mendez-Santiago–Teja model and Sung–Shim model

Chrastil model	k	α	β	AARD (%)
Water	1.46	−2914.37	0.36	3.36
Acid Red 138	1.46	−2806.11	0.25	8.58
Mendez-Santiago–Teja model	A'	B'	C'	AARD (%)
Water	−4924.31	1.28	17.63	3.03
Acid Red 138	−4622.72	1.16	15.83	6.06

Sung–Shim model	A	B	C	D	AARD (%)
Water	17.88	−6876.09	−1.09	628.05	2.91
Acid Red 138	9.55	−3668.29	−0.05	154.91	5.19

3.3 Effect of experimental parameters on the solubilities of Acid Red 138 with water co-solvent

Effect of carbon dioxide pressure on the mole fraction (y_2) of Acid Red 138 in supercritical carbon dioxide with water is presented in Fig. 4. As shown, with pressure increasing from 20 to 26 MPa, the solubilities of Acid Red 138 increased moderately in supercritical carbon dioxide. It is also observed that Acid Red 138 solubility enhanced as the carbon dioxide temperature increased between 353.15 K and 413.15 K. Moreover, the growth trends of dye solubility were consistent with the increasing trends of water since the density of carbon dioxide increases. It is thus proved that the solubilities of the Acid Red 138 were improved in supercritical carbon dioxide, which can be attributed to the increase of the carbon dioxide polarity under the action of water.[26,33] An improvement for the solubilities of Acid Red 138 was also exhibited with system pressure rising from 20 to 26 MPa at a constant temperature, which can be attributed to more water dissolving as temperature increased. Moreover, as
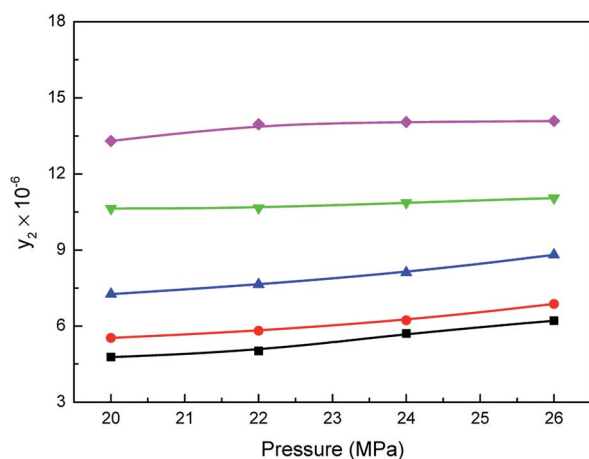
listed in Table S3,† the dye concentrations in liquid phase decreased as carbon dioxide temperature and pressure increasing, which presents the opposite trend in comparison with the increase of the dye solubility in supercritical carbon dioxide.

3.4 Correlation of the experimental solubility data

Generally, there are various mathematical models which can be used to correlate solute solubility data in supercritical carbon dioxide. Of which empirical models are the most widely used due to their excellent accuracy and applied range.[34] In this study, Chrastil model (seen in eqn (3)), Mendez-Santiago–Teja model (seen in eqn (4)) as well as Sung–Shim model (seen in eqn (5)) were employed to predict the solubility of water and Acid Red 138.[31,35–37]

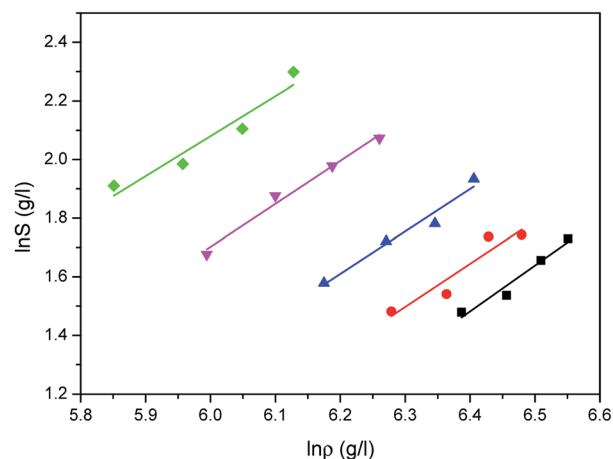$$\ln S = k \ln \rho + \frac{\alpha}{T} + \beta \qquad (3)$$

Fig. 4 Relationship between the solubilities of Acid Red 138 in supercritical CO_2 saturated with water and the pressure: ■ -353.15 K, ● -363.15 K, ▲ -373.15 K, ▼ -393.15 K, ◆ -413.15 K.

Fig. 5 Correlated results of water solubility S against ρ from the Chrastil model: ◆ -353.15 K, ▼ -363.15 K, ▲ -373.15 K, ● -393.15 K, ■ -413.15 K, – calculated.
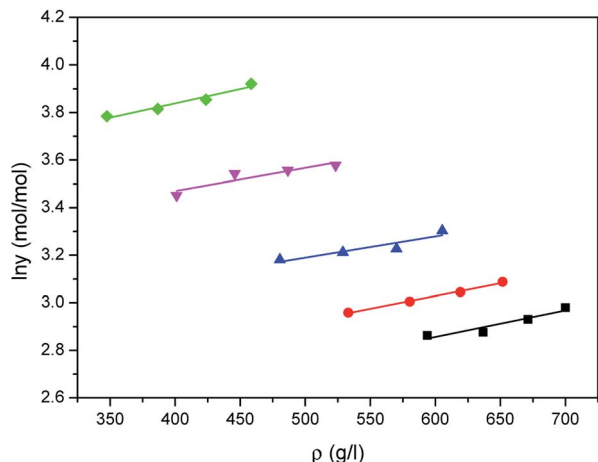
Fig. 6 Correlated results of water solubility y against ρ from the Mendez-Santiago–Teja model: ◆ -353.15 K, ▼ -363.15 K, ▲ -373.15 K, ● -393.15 K, ■ -413.15 K, – calculated.

Fig. 8 Correlated results of solubility S of Acid Red 138 in supercritical CO_2 saturated with water against ρ from the Chrastil model: ◆ -353.15 K, ▼ -363.15 K, ▲ -373.15 K, ● -393.15 K, ■ -413.15 K, – calculated.

where S (g l^{-1}) refers to the solubility of solute in supercritical fluid; ρ (kg m^{-3}) refers to the pure supercritical fluid density; α and β are constants, and k is the association number.

$$T\ln(yp) = A' + B'\rho + C'T \tag{4}$$

where y refers to the solute solubility in supercritical fluid; A', B', and C' are constants.

$$\ln y = A + \frac{B}{T} + \left(C + \frac{D}{T}\right)\ln\rho \tag{5}$$

where A, B, C and D are constants.

The average absolute relative deviation (AARD) between the calculated solubilities (y^{cal}) and the experimental solubility (y^{exp}) is calculated according to eqn (6).[38]

$$\text{AARD }(\%) = \frac{100}{N}\sum_{n}\frac{|y^{cal} - y^{exp}|}{y^{exp}} \tag{6}$$
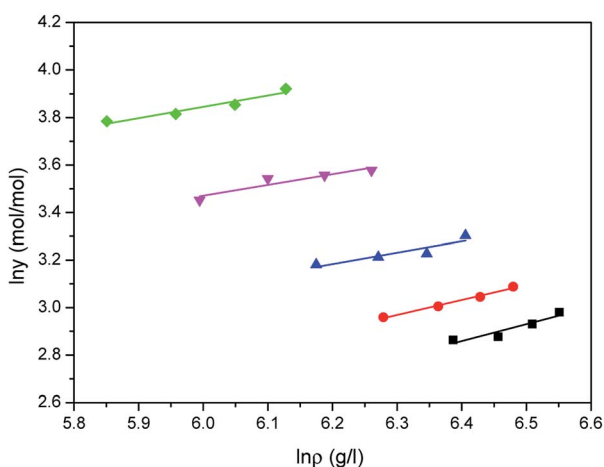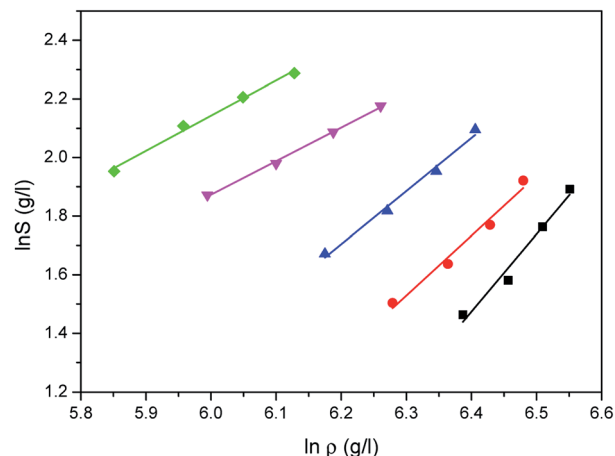
where N refers to the data points number.

The parameters of Chrastil model, Mendez-Santiago–Teja model and Sung–Shim model are listed in Table 2. It can be seen that AARD values of water were 3.36%, 3.03% and 2.91% for Chrastil equation, Mendez-Santiago–Teja equation and Sung–Shim equation while those values for Acid Red 138 were 8.58%, 6.06% and 5.19%, respectively. The obtained results showed that the AARD values presented excellent fitting effect whereas Sung–Shim equation indicates better correlation function because of more adjustable parameters employed.

Comparison results between the experimental solubilities of water and the correlated data are illustrated in Fig. 5–7, respectively. Compared to Sung–Shim model, less satisfactory prediction results under lower and higher density conditions are displayed with Chrastil model and Mendez-Santiago–Teja model. This phenomenon may mean that a phase behavior change of water occurs at lower or higher temperature.[39]
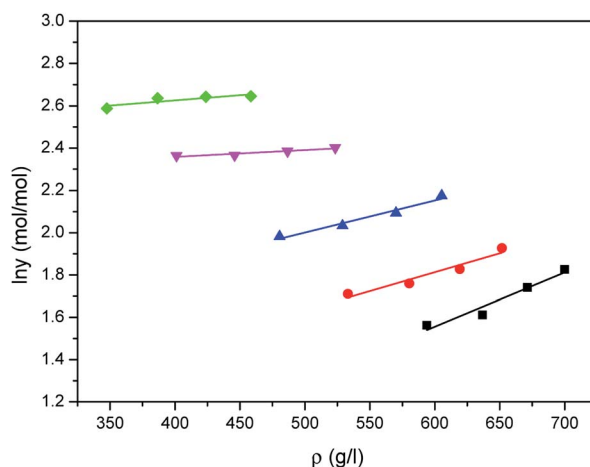

Fig. 7 Correlated results of water solubility y against ρ from the Sung–Shim model: ◆ -353.15 K, ▼ -363.15 K, ▲ -373.15 K, ● -393.15 K, ■ -413.15 K, – calculated.

Fig. 9 Correlated results of solubility y of Acid Red 138 in supercritical CO_2 saturated with water against ρ from the Mendez-Santiago–Teja model: ◆ -353.15 K, ▼ -363.15 K, ▲ -373.15 K, ● -393.15 K, ■ -413.15 K, – calculated.
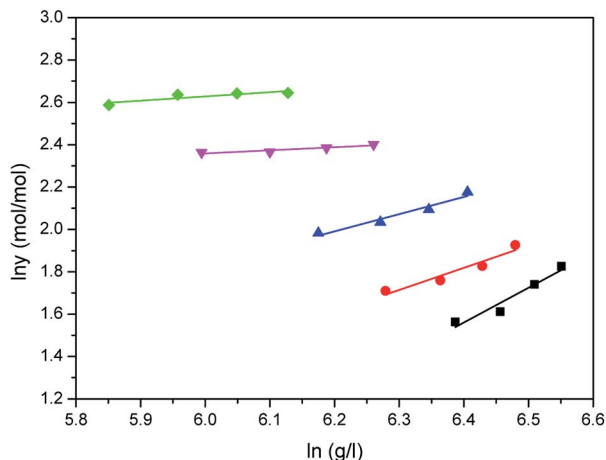
Fig. 10 Correlated results of solubility *y* of Acid Red 138 in supercritical CO$_2$ saturated with water against ρ from the Sung–Shim model: ◆ -353.15 K, ▼ -363.15 K, ▲ -373.15 K, ● -393.15 K, ■ -413.15 K, – calculated.

The correlated results of solubility for Acid Red 138 against ρ are illustrated in Fig. 8–10, respectively. As shown, the Chrastil equation, Mendez-Santiago–Teja equation and Sung–Shim equation gave a less satisfactory prediction results in comparison with those of water. The cause of this phenomenon may be duo to the complexity of the supercritical carbon dioxide-water-dye system after Acid Red 138 was added.[40] But, the AARD values for Acid Red 138 were within 10%, which demonstrated that the fitting effects of the two models were acceptable.

4   Conclusions

Solubilities of water and Acid Red 138 with water as co-solvent in supercritical carbon dioxide were measured from 20 to 26 MPa at different temperatures (353.15, 363.15, 373.15, 393.15 and 413.15 K). It is found that the solubilities of water and Acid Red 138 solution increased gradually with the rising pressure at a constant system temperature. Simultaneously, the solubilities of Acid Red 138 increased with system temperature and pressure increasing due to more water dissolving at supercritical carbon dioxide dyeing conditions. The experimental solubility data of water and Acid Red 138 were also correlated successfully with Chrastil empirical model, Mendez-Santiago–Teja empirical model and Sung–Shim empirical model with the AARD values of 3.36%, 3.03%, 8.58%, 6.06%, 2.91% and 5.19%. Enhancing the solubility of Acid Red 138 in supercritical carbon dioxide by adding water will provide basic data for the construction of new microemulsion for natural fibers dyeing, which may offer an alternative for industrialization of natural fibers dyeing in supercritical carbon dioxide.

Conflicts of interest

There are no conflicts to declare.

References

1 J. Zhang, B. Han, J. Li, Y. Zhao and G. Yang, *Angew. Chem., Int. Ed.*, 2011, **50**, 9911–9915.
2 Z. Liu, J. Chen, Z. Liu and J. Lu, *Macromolecules*, 2008, **41**, 6987–6992.
3 H. Zheng, J. Zhang, J. Yan, X. Xiong, H. Zhao and L. Zheng, *RSC Adv.*, 2017, **7**, 3470–3479.
4 W. Leitner, *Acc. Chem. Res.*, 2002, **35**, 746–756.
5 M. Li, L. Liu, X. Huang, H. Liu, B. Chen, L. Guan and Y. Wu, *RSC Adv.*, 2017, **7**, 49817–49827.
6 B. Kueh, S. Yusup and N. Osman, *J. CO$_2$ Util.*, 2018, **24**, 220–227.
7 J. Liu, B. Han, Z. Wang, J. Zhang, G. Li and G. Yang, *Langmuir*, 2002, **18**, 3086–3089.
8 A. E. Polloni, J. G. Veneral, E. A. Rebelatto, D. D. Oliveira, J. V. Oliveira, P. H. H. Araújo and C. Sayer, *J. Supercrit. Fluids*, 2017, **119**, 221–228.
9 Y. Iwai, H. Nagano, G. S. Lee, M. Uno and Y. Arai, *J. Supercrit. Fluids*, 2006, **38**, 312–318.
10 H. Zheng, Y. Xu, J. Zhang, X. Xiong, J. Yan and L. Zheng, *J. Cleaner Prod.*, 2017, **143**, 269–277.
11 J. Long, C. Cui, Y. Zhang and G. Yuan, *Dyes Pigm.*, 2015, **115**, 88–95.
12 T. A. Elmaaty, J. Ma, F. El-Taweel, E. A. Elaziz and S. Okubayashi, *Ind. Eng. Chem. Res.*, 2014, **53**, 15566–15570.
13 T. A. Elmaaty and E. A. Elaziz, *Text. Res. J.*, 2017, **88**, 1184–1212.
14 H. Zheng, J. Zhang, J. Yan and L. Zheng, *J. CO$_2$ Util.*, 2016, **16**, 272–281.
15 S. G. Kazarian, M. F. Vincent, B. L. West and C. A. Eckert, *J. Supercrit. Fluids*, 1998, **13**, 107–112.
16 M. V. D. Kraan, M. V. F. Cid, G. F. Woerlee, W. J. T. Veugelers, C. J. Peters and G. J. Witkamp, *J. Supercrit. Fluids*, 2007, **40**, 336–343.
17 D. Aslanidou, C. Tsioptsias and C. Panayiotou, *J. Supercrit. Fluids*, 2013, **76**, 83–93.
18 H. Zheng, J. Zhang, M. Liu, J. Yan, H. Zhao and L. Zheng, *J. CO$_2$ Util.*, 2017, **18**, 117–124.
19 S. Sarrade, D. Féron, F. Rouillard, S. Perrin, R. Robin, J. Ruiz and H. Turc, *J. Supercrit. Fluids*, 2017, **120**, 335–344.
20 A. Sabirzyanov, A. Il'in, A. Akhunov and F. Gumerov, *High Temp.*, 2002, **40**, 203–206.
21 M. King, A. Mubarak, J. Kim and T. Bott, *J. Supercrit. Fluids*, 1992, **5**, 296–302.
22 F. Tabasinejad, R. Moore, S. Mehta, K. Fraassen and Y. Barzin, *Ind. Eng. Chem. Res.*, 2011, **50**, 4029–4041.

23 P. Muthukumaran, R. B. Gupta, H. D. Sung, J. J. Shim and H. K. Bae, *Korean J. Chem. Eng.*, 1999, **16**, 111–117.

24 C. C. Tsai, H. M. Lin and M. J. Lee, *J. Chem. Eng. Data*, 2009, **54**, 1442–1446.

25 A. Özcan and A. S. Özcan, *Fluid Phase Equilib.*, 2006, **249**, 1–5.

26 J. Zhang, H. Zheng and L. Zheng, *J. Nat. Fibers*, 2018, **15**, 1–10.

27 A. Bamberger, G. Sieder and G. Maurer, *J. Supercrit. Fluids*, 2000, **17**, 97–110.

28 NIST, National Institute of Standards and Technology, http://webbook.nist.gov/chemistry/fluid/, accessed 15.04.19.

29 C. Jiang, Z. Sun, Q. Pan and J. Pi, *J. Chem. Eng. Data*, 2012, **57**, 1794–1802.

30 M. Artal, V. Pauchon, J. M. Embid and J. Jose, *J. Chem. Eng. Data*, 1998, **43**, 983–985.

31 J. Chrastil, *J. Phys. Chem.*, 1982, **86**, 3016–3021.

32 Z. Wang, Q. Zhou, H. Guo, P. Yang and W. Lu, *Fluid Phase Equilib.*, 2018, **476**, 170–178.

33 M. V. D. Kraan, M. V. F. Cid, G. F. Woerlee, W. J. T. Veugelers, C. J. Peters and G. J. Witkamp, *J. Supercrit. Fluids*, 2007, **40**, 336–343.

34 L. Manna and M. Banchero, *J. Chem. Eng. Data*, 2018, **63**, 1745–1751.

35 P. Coimbra, M. R. Blanco, H. S. R. C. Silva, M. H. Gil and H. C. D Sousa, *J. Chem. Eng. Data*, 2006, **51**, 1097–1104.

36 K. C. Pitchaiah, N. Sivaraman, N. Lambab and G. Madras, *RSC Adv.*, 2016, **6**, 51286–51295.

37 S. Yoda, Y. Mizuno, T. Furuya, Y. Takebayashi, K. Otake, T. Tsuji and T. Hiaki, *J. Supercrit. Fluids*, 2008, **44**, 139–147.

38 K. Tamura and R. S. Alwi, *Dyes Pigm.*, 2015, **113**, 351–356.

39 J. Zheng, M. Xu, X. Lu and C. Lin, *Chin. J. Chem. Eng.*, 2010, **18**, 648–653.

40 J. Zhang, H. Zheng and L. Zheng, *Text. Res. J.*, 2018, **88**, 155–166.